



FACILITY FORM 802

N65-25012

(ACCESSION NUMBER)

(THRU)

(PAGES)

(CODE)

(NASA CR OR TMX OR AD NUMBER)

(CATEGORY)

46  
CR 62933

1  
13

GPO PRICE \$ \_\_\_\_\_

OTS PRICE(S) \$ \_\_\_\_\_

Hard copy (HC) 2.00

Microfiche (MF) 50

# ERROR ANALYSIS ON INVERSION TECHNIQUES

JEAN I. F. KING



Bedford, Massachusetts

---

INTERIM SCIENTIFIC REPORT NO. 1  
Covering the period 23 May 1963 - 30 November 1964  
CONTRACT NO. NAS5-3352

---

PREPARED FOR  
NATIONAL AERONAUTICS AND SPACE ADMINISTRATION  
GODDARD SPACE FLIGHT CENTER  
GREENBELT, MARYLAND

GCA Technical Report No. 64-16-N

ERROR ANALYSIS ON INVERSION TECHNIQUES

Jean I. F. King

INTERIM SCIENTIFIC REPORT NO. 1

Covering the period 23 May 1963 - 30 November 1964

Contract No. NAS5-3352

November 1964

GCA CORPORATION  
GCA TECHNOLOGY DIVISION  
Bedford, Massachusetts

Prepared for

NATIONAL AERONAUTICS AND SPACE ADMINISTRATION  
Goddard Space Flight Center  
Greenbelt, Maryland

ABSTRACT

25012

This final report documents the progress towards the Contract goal of finding an optimum inversion technique for inferring vertical thermal structure from satellite infrared observations. The major part of the research under Contract has appeared in the scientific literature. These articles are appended to the text. The final report consists therefore of a running commentary detailing our ideas as the understanding of the problem deepened. We conclude with unpublished material which tests the new inversion method under random observational errors.

*Author*

TABLE OF CONTENTS

<u>Section</u>	<u>Title</u>	<u>Page</u>
	ABSTRACT	i
1	INTRODUCTION	1
2	THEORY	4
APPENDIX A	MOMENT METHOD FOR SOLUTION OF THE SCHWARZSCHILD-MILNE INTEGRAL EQUATION	20
APPENDIX B	GREENHOUSE EFFECT IN A SEMI-INFINITE ATMOSPHERE	21
APPENDIX C	RADIATIVE TRANSFER WITH IMBEDDED SOURCES	22
APPENDIX D	INVERSION BY SLABS OF VARYING THICKNESS	26

LIST OF ILLUSTRATIONS

<u>Figure</u>	<u>Title</u>	<u>Page</u>
1	Inferred five-slab atmosphere	15
2	Inferred atmosphere with four-decimal observation accuracy	17
3	Inferred atmosphere with three-decimal observation accuracy	18
4	Inferred atmosphere with two-decimal observation accuracy	19

## SECTION 1

### INTRODUCTION

With the advent of the TIROS series meteorologists had for the first time a platform for topside viewing of the atmosphere. In the visible this consists largely of scattered sunlight, hence the interest in cloud patterns for what they reveal of the wind velocity field. Unfortunately, the scattered sunlight is largely insensitive to the thermal and pressure structure of the atmosphere.

The mean terrestrial temperature around 285K, with the maximum of the Planck emission centered near 15 microns, suggests using the infrared region for thermal sensing. Since certain atmospheric constituents ( $\text{CO}_2, \text{H}_2\text{O}, \text{O}_3$ ) are infrared active, they will appear as absorption bands imposed on the black-body background continuum of the earth. If the bands are sufficiently opaque the satellite will intercept photons arising solely from the top of the, say, water vapor layer whose intensity is given by the Planck function associated with that particular temperature and frequency.

These considerations bracket the problem. If we look in a window ( $\kappa \rightarrow 0$ ) we will see infinitely deep into the atmosphere, in our case the surface temperature. At the other viewing extreme of an opaque band center ( $\kappa \rightarrow \infty$ ), only the temperature of the top of the emitting layer will be

sensed. The question poses itself: Is it possible to determine intermediate temperatures between these levels by viewing the intermediate frequencies?

The relation stating the radiation frequency dependence on vertical thermal structure follows from transfer theory as

$$I(\kappa) = \int_0^{\infty} B(u) e^{-\kappa u} \kappa \, du \quad , \quad (1)$$

Where B is the Planck intensity and  $\exp(-\kappa u)$  the transmittance. This model assumes a plane-parallel atmosphere viewed vertically at varying monochromatic frequencies. By concentrating on this geometry we gain greatly in mathematical simplicity while losing little in principle. Thus using Equation (1) we arrive at once to the bracketing values of the deep and topside intensities

$$\begin{aligned} \lim_{\kappa \rightarrow 0} I(\kappa) &= \lim_{\kappa \rightarrow 0} \left[ B(0) + \int_0^{\infty} \frac{dB(u)}{du} e^{-\kappa u} \, du \right] \\ &= B(0) + B(\infty) - B(0) = B(\infty) \end{aligned} \quad (2)$$

and

$$\begin{aligned} \lim_{\kappa \rightarrow \infty} I(\kappa) &= \lim_{\kappa \rightarrow \infty} \int_0^{\infty} B(u) e^{-\kappa u} \kappa \, du \\ &= \int_0^{\infty} B(u) \delta(u) \, du = B(0) \quad . \end{aligned}$$

Equation (1) states that the intensity  $I(\kappa)$  is the moment of the

Planck intensity weighted by the transmittance derivative

$$w(u) = \int_0^\infty \kappa e^{-\kappa u} d\kappa \quad (3)$$

Since  $w(u)$  decreases monotonically with depth  $u$ , this implies a strong weighting of the near field, i.e. the top of the atmosphere. These considerations set the limits on temperature inference. The near field weighting indicates increasing unreliability of deep thermal sensing. Further we are asked to construct a thermal profile from a knowledge of its moments. This is similar to asking the distribution of grades on an exam given only certain averages.

Formally, at least, since Equation (1) is a Laplace transform the solution follows from the inversion theorem as

$$B(u) = \frac{1}{2\pi i} \int_{\gamma-i\infty}^{\gamma+i\infty} \frac{I(\kappa)}{\kappa} e^{\kappa u} d\kappa \quad (4)$$

Of course if the intensity were known continuously and exactly, there would be no problem since the temperature profile would be uniquely specified. In practice, however, the intensity is sensed at the finite number of channels within a band. The inversion problem then consists of extracting the maximum amount of thermal information from these intensity observations.



## SECTION 2

### THEORY

We are now in a position to state the inversion problem: Given  $n$  discrete values of an intensity profile,

$$I_i = I(\kappa_i) \quad , \quad i = 1, 2, \dots, n \quad (5)$$

deduce the atmosphere which gives rise to the observations. This problem as it stands does not have a unique solution. Any single-valued intensity curve passing through the observations gives, upon inversion, an allowable solution. Since there is a non-denumerable infinity of such curves, there is a corresponding infinity of temperature patterns fitting the data. Many of these profiles fluctuate wildly with grossly superadiabatic lapse-rates and even negative temperatures. This is evidence that we must impose some constraint to reduce the number of possible solutions.

There are two ways of approaching the constraint. The first led by physical argument to the imbedded source technique. The second method, inversion by slabs of varying thickness, was arrived at by mathematical considerations of smoothness in the curve-fitting.

Research during the first half of the contract period centered on the imbedded source technique, which we now discuss. As we have seen, Equation (4) is an incomplete statement of the inversion problem since there is no discrimination between unphysical and feasible solutions. Both the observed intensity and temperature structure are end results or effects of deeper causes. Thus one is led naturally to attempt to relate the two effects to an underlying cause, rather than directly to each other. These considerations gave rise to the imbedded source technique. The temperature distribution is in a real sense determined uniquely by the strength and character of the radiation incident on the atmosphere boundaries and the distribution and concentration of absorbing gases within.

Formally the solution involved three steps: First radiative transfer theory was used to relate the upwelling intensity with the transform of the imbedded sources, then an inversion was performed to obtain this source distribution. Finally transfer theory was again used to obtain the temperature distribution associated with the imbedded source. Schematically, the process may be written

$$\begin{array}{ll}
 \text{I} & I(0, \mu_i) \rightarrow \mathcal{S}(1/\mu_i) \\
 \text{II} & \mathcal{S}(1/\mu_i) \rightarrow S(\tau) \\
 \text{III} & S(\tau) \rightarrow B(\tau)
 \end{array} \tag{6}$$

The critical step is the second one, the inversion. We have a partial

knowledge beforehand of the strength of the external radiation fields and the absorbing gases which constitute the imbedded sources. Certain constraints follow naturally. The flux, for instance, must fall off continuously as the medium is penetrated.

The imbedded source technique led to two results:

1) An understanding of the connection between radiative sources and sinks and the vertical temperature profile. Thus three, and possibly five papers, were stimulated by this approach to radiative transfer.

2) The failure of the imbedded source technique to solve satisfactorily the inversion problem led to the formulation of the method of variable slab thickness.

The first paper to appear under contract "Moment Method for Solution of the Schwarzschild-Milne Integral Equation" (see Appendix A) solved the equilibrium transfer equation by approximating the exponential integral equation kernel with a finite sum of exponential functions. Although developed in the context of the equilibrium problem, this moment method had the flexibility for application to more general problems to follow.

The first application of the imbedded source technique appeared as the "Greenhouse Effect in a Semi-Infinite Atmosphere" (see Appendix B). The vertical thermal profile of a planetary atmosphere heated from above was calculated. In the model the imbedded heat source, due to direct absorption of sunlight was assumed to fall off exponentially with in-

creasing depth. Through this model one was able to relate the thermal profile directly to a greenhouse factor

$$\mu_0 = \frac{\kappa_{ir}}{\kappa_{vis}} \quad (7)$$

defined as the ratio of the infrared to visible absorption coefficients. The quantitative results in general agreed with qualitative intuition, e.g. the higher the greenhouse factor, the higher the temperature at large depths. Of surprise, however, was the compensatory greenhouse "cooling" aloft with increasing infrared opacity. This special model gave one general result of great interest. It would appear that the lowest possible free-air temperature of an externally heated planetary atmosphere is given by

$$\frac{T_{min}}{T_{eff}} = \left( \frac{B_{min}}{B_{eff}} \right)^{1/4} = \left( \frac{3}{16} \right)^{1/8} \quad (8)$$

Applied to the terrestrial atmosphere, this predicts that the tropical stratosphere is close to this minimum obtainable temperature.

In this paper the generalized Schwarzschild-Milne integral equation

$$B(\tau) = S(\tau) + \frac{1}{2} \int_0^{\infty} B(t) E_1(|t-\tau|) dt \quad (9)$$

was solved for an exponential source

$$S(\tau) = e^{-\tau/\mu_0}/\mu_0 \quad (10)$$

It would be advantageous to be able to solve this equation, i.e. the temperature profile for an arbitrary array of imbedded sources. This proves possible using a modified Wiener-Hopf technique to obtain the following Green's function solution for the problem

$$\begin{aligned}
 G(\tau|\tau_1) = G(\tau_1|\tau) = & 3\eta(\tau_1-\tau) \left[ \tau+q(\tau)+q(\tau_1)+q(\tau_1-\tau) \right. \\
 & \left. + \frac{q'}{\sqrt{3}} (\tau_1-\tau) + \int_0^\tau q'(\tau_1-t)q'(\tau-t)dt \right] + \delta(\tau-\tau_1) \\
 & + 3\eta(\tau-\tau_1) \left[ \tau_1+q(\tau_1) + q(\tau) - q(\tau-\tau_1) \right. \\
 & \left. + \frac{q'}{\sqrt{3}} (\tau-\tau_1) + \int_0^{\tau_1} q'(\tau_1-t)q'(\tau-t)dt \right] ,
 \end{aligned} \tag{11}$$

where  $q(\tau)$  and  $\eta(\tau)$  are the Hopf function and the Heaviside step function. A knowledge of the Green's function reduces the solution of Equation (9) to simple quadrature via the prescription

$$B(\tau) = \int_0^\infty S(\tau_1)G(\tau|\tau_1)d\tau_1 . \tag{12}$$

In a comprehensive paper being prepared for publication in the Astrophysical Journal, the solution of Schwarzschild-Milne equation (9) is obtained for a variety of imbedded sources. For an outline of the contents see Appendix C. The meteorological consequences of various models have been presented as two invited papers. The first, "Radiative Transfer with Imbedded Sources", read at the recent Radiation Symposium in Leningrad used a double imbedded source which yielded many features of the

standard atmosphere. Particularly satisfying was the prediction of a tropopause-like temperature minimum at a depth of one-quarter atmosphere (250 mbs). An increase in the infrared optical thickness resulted in raising the height and lowering the temperature of the tropopause which was very suggestive of tropical behavior.

More recently further implications of the imbedded source technique were presented at the AMS Micrometeorology Conference in a paper "The Nature of the Radiative Discontinuity Near the Ground". The theory makes the startling prediction that the upwelling infrared radiation from a dry, smooth surface should be anisotropic, exhibiting limb-brightening.

The imbedded source technique, while contributing to the understanding of the inversion problem, did not provide its solution. To appreciate the limitations of the imbedded source technique and to see the considerations which led to the variable slab method, we must return to Equation (4)

$$B(u) = \frac{1}{2\pi i} \int_{\gamma-i\infty}^{\gamma+i\infty} \frac{I(\kappa)}{\kappa} e^{\kappa u} d\kappa \quad (4)$$

The natural forms for expressing imbedded sources are exponential functions

$$S(\tau) = C_1 e^{-\tau/\mu_0}, C_2 e^{-(\tau_1 - \tau)/\mu_0} \quad (13)$$

either decreasing or increasing with depth depending on whether the source is above or below. The upwelling radiation corresponding to

sums of exponential sources has a quotient polynomial form

$$I(\kappa) = \frac{a_n \kappa^n + a_{n-1} \kappa^{n-1} + \dots + a_0}{b_n \kappa^n + b_{n-1} \kappa^{n-1} + \dots + b_0} \quad (14)$$

This then is the interpolation formula for the upwelling intensity. The constants  $a_i$  and  $b_i$  are determined by fitting the  $2n + 2$  observations, Equation (5)

$$I_i = I(\kappa_i) \quad , \quad i = 1, 2, \dots, 2n + 2 \quad (5)$$

Unfortunately, when this procedure is applied to a routine model it is found that the fit with observations requires either negative or complex roots for  $\kappa$ , which is physically inadmissible. This indicates that a quotient polynomial interpolation formula is suitable for slowly varying sources, but incapable of dealing with sources which change abruptly.

In this manner we were led to the following temperature profile of extreme "bumpiness" as the source

$$\frac{dB(u)}{du} = \sum_{j=1}^n \Delta B_j \delta(u-u_j) \quad , \quad (15)$$

from which follows as the interpolation formula

$$\begin{aligned} I(\kappa) - B(0) &= \int_0^{\infty} \frac{dB(u)}{du} e^{-\kappa u} du \\ &= \sum_{j=1}^n \Delta B_j e^{-\kappa u_j} \end{aligned} \quad (16)$$

Using the observational constraint, Equation (5) , we have a nonlinear simultaneous equation set in  $2n$  unknowns  $\Delta B_j$  and  $u_j$  to determine

$$I(\kappa_i) - B(0) = \sum_{j=1}^n \Delta B_j e^{-\kappa_i u_j} \quad i=1,2,\dots,2n \quad . \quad (17)$$

It is indeed fortunate that this non-linear set can be solved, uniquely, by an elegant algorithm which determines the  $n$  slab boundaries  $u_j$  as the roots of an  $n$ th degree algebraic equation and the slab weights  $\Delta B_j$  as the solutions of  $n$  linear simultaneous equations. The uniqueness feature should be stressed. For  $2n$  intensity observations there is one and only one configuration of  $n$  slabs of varying heights and thicknesses which fit the observations. Thus this method is free of the indeterminacy which plagues other interpolation formulas. An example will suffice.

Let us assume we wish to express the temperature as a power series

$$B(u) = \sum_{j=0}^n b_j u^j \quad . \quad (18)$$

By taking the transform we obtain as our interpolation formula

$$I(\kappa) = \sum_{j=0}^n \frac{j! b_j}{\kappa^j} \quad . \quad (19)$$

The observational fit requires

$$I(\kappa_i) = \sum_{j=0}^n \frac{j! b_j}{\kappa_i^j} \quad . \quad (20)$$



The power series specifies the sequence  $j=0,1,2,\text{etc.}$ . Thus  $\kappa_i^j$  is known and Equation (20) becomes a linear simultaneous set for the unknowns  $b_j$ . But what if another sequence had been chosen, such as  $j=0,2,4$ , for example? This would have led to the inference of a different profile, with no ready criterion to favor one over the other.

The paper "Inversion by Slabs of Varying Thickness" (see Appendix D) sets forth the theory and applies the new method to two synthetic models. The inferred fit is convincing, and subsequent work has justified our early optimism in this new method.

Thus far we have not mentioned one problem of overriding importance to all inversion methods. This is the effect of noisy data on the inferred temperature. To this point we have discussed only the problem: Given perfect data, i.e. free from error, which is the best inversion scheme? Perhaps the chief virtue of the variable slab method is its stability to error. This we proceed to demonstrate by numerical examples of work done under contract which is as yet unpublished in the literature.

In the first model studied in the "Inversion by Slabs of Varying Thickness" paper, the indicial function which we sought to reclaim was given by

$$B(u) = 1 - e^{-\kappa_0 u} \quad (21)$$

and the corresponding upwelling radiation by its transform

$$I(\kappa) = \frac{1}{1 + \frac{\kappa}{\kappa_0}} \quad (22)$$

If we view the atmosphere at ten frequencies corresponding to

$$\frac{\kappa_i}{\kappa_0} = 0, 1, 2, \dots, 9, \quad (23)$$

then the upwelling radiation strengths will be given by the sequence

$$I(\kappa_i) = 1, 1/2, 1/3, \dots, 1/9, 1/10 \quad (24)$$

This array suggests a way in which we can determine the sensitivity of the inferred slab profile to observational errors. From ten exact measurements we should be able to deduce a five slab atmosphere whose profile closely approximates the indicial function Equation (21). Figure 1 displays the five slab profile deduced from perfect data. The fit is extraordinarily good. Table 1 lists the slab parameters inferred from the perfect data, Equation (24) along with slab parameters inferred from values of  $I(\kappa_i)$  rounded off to eight places. We see the effect of eighth place data round-off is to give rise to a maximum inferred error of five in the fourth decimal place. From a graphical point of view this is negligible, smaller than the width of a line.

Let us now successively degrade the data by rounding off to fewer decimal places and observe the resulting deterioration of the

TABLE 1

## INFERRED FIVE-SLAB ATMOSPHERE

## A. Exact Solution

j	$B_j$	$x_j$	$\tau_j$
1	.11846344	.95308992	.048
2	.35777778	.76923466	.262
3	.64222222	.50000000	.693
4	.88153656	.23076534	1.47
5	1.00000000	.04691008	3.06

## B. Approximate Solution for Eight-Decimal Accuracy

1	.11822508	.95318628	.048
2	.35715669	.76966538	.262
3	.64143363	.50073967	.692
4	.88108260	.23142699	1.46
5	.99999997	.04710907	3.06

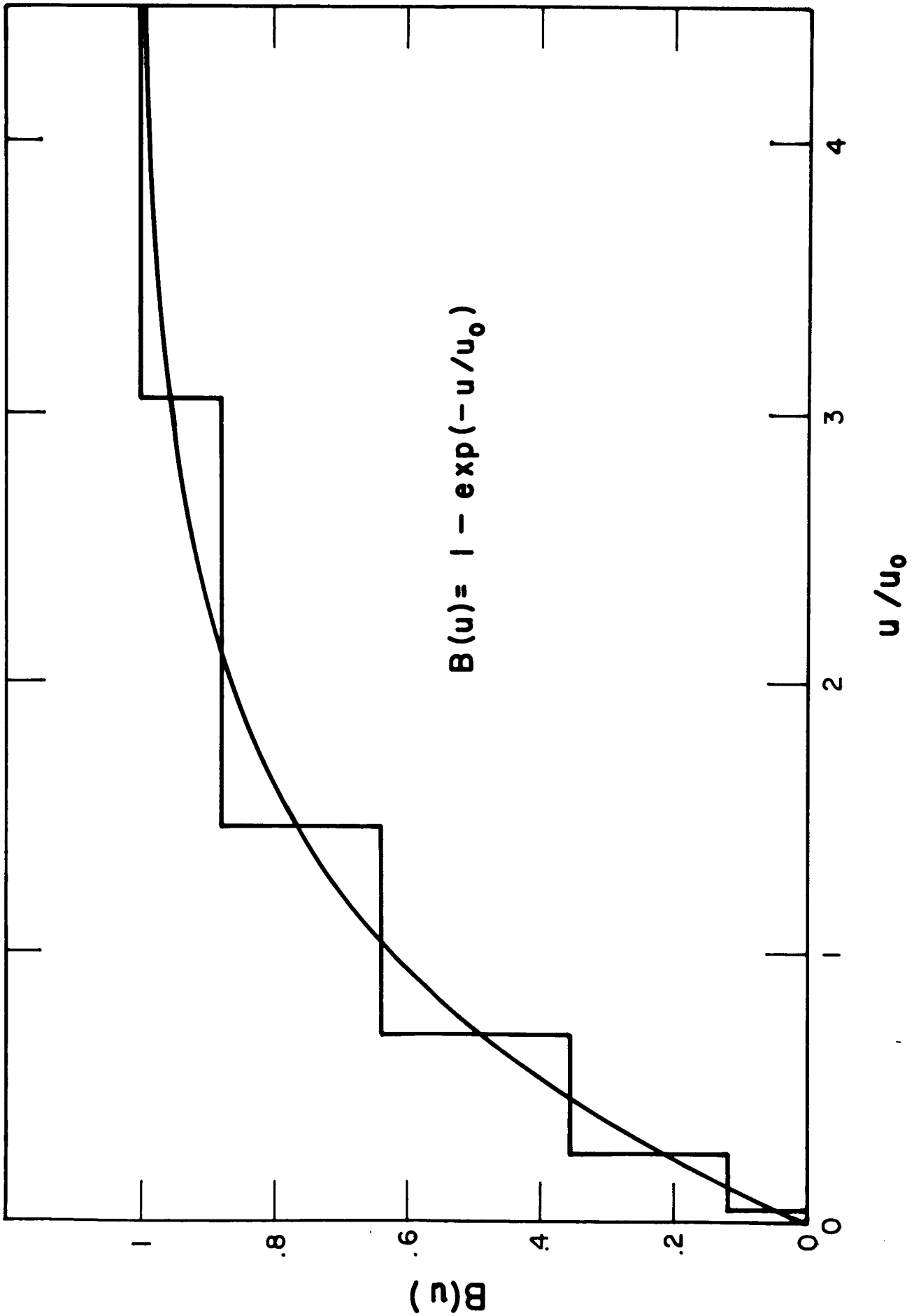


Figure 1. Inferred five-slab atmosphere.

inferred thermal profile. Figure 2 shows the effects of four decimal round-off. The smallest root  $x_5$  goes negative but the associated  $\Delta B_5$  is comfortingly small. Thus we have, in effect, lost a slab. The shape of the inferred profile is unaltered, and what remains is an excellent four slab reconstruction of the indicial function.

With three place round-off the degradation progresses further. Figure 3 shows that two slabs are lost, with  $x_1 > 1$  corresponding to a negative  $\tau_1$  of  $-.764$ . Two decimal round-off introduces the new feature that two of the roots  $x_4$  and  $x_5$  become a complex conjugate pair. The associated  $\Delta B_4$  and  $\Delta B_5$  are, however, extremely small. Once again the shape of the profile is faithfully reproduced (see Figure 4), though necessarily with the less precision of three slabs.

These results are reassuring. They appear to indicate an extreme stability of the profile shape to non-systematic error. Of further interest is the fact that the smallest root  $x_5$  is most sensitive to error. This corresponds to large  $\tau$ , i.e. deep in the atmosphere, where we would expect maximum unreliability anyway in thermal reconstruction.

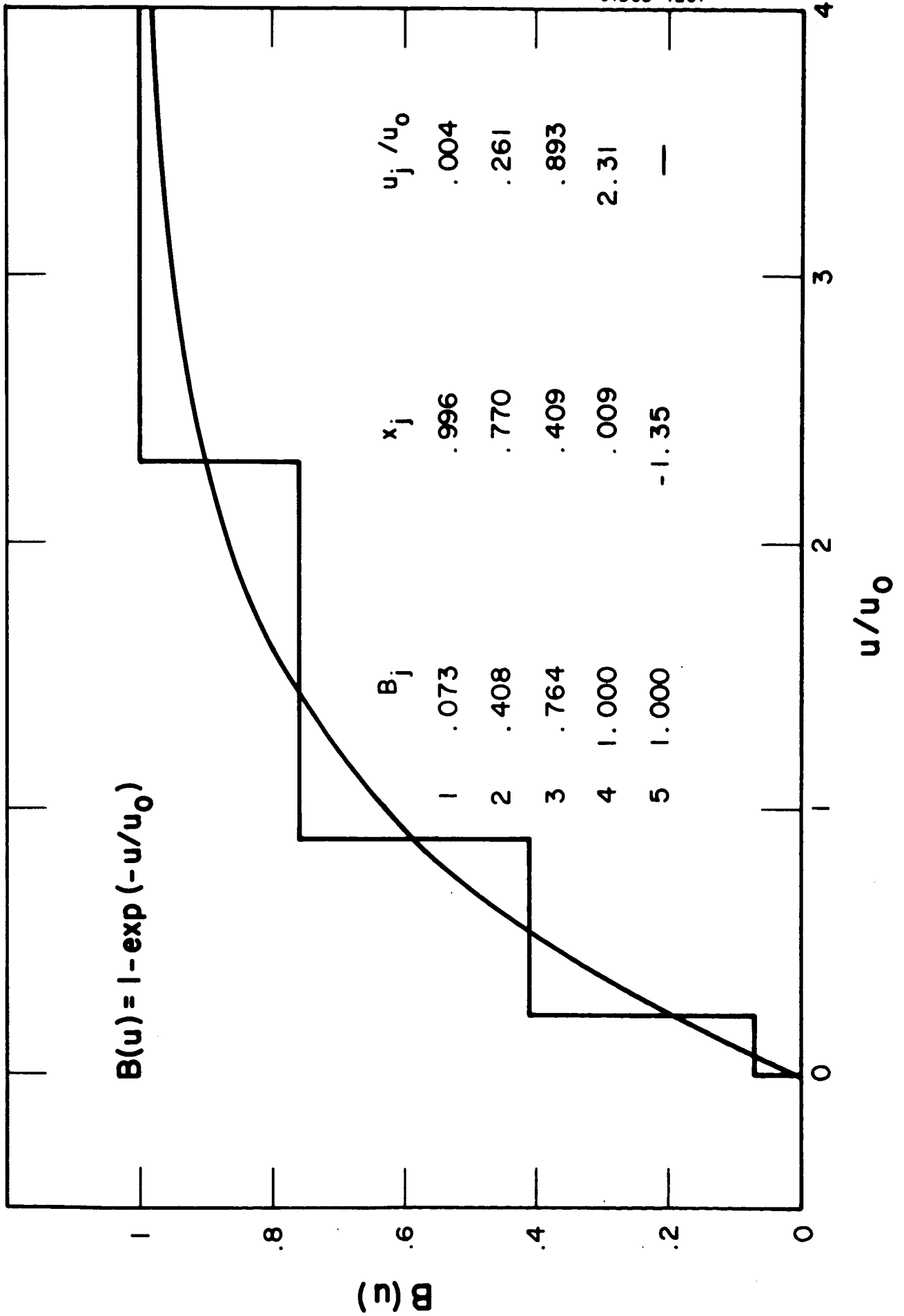


Figure 2. Inferred atmosphere with four-decimal observation accuracy.

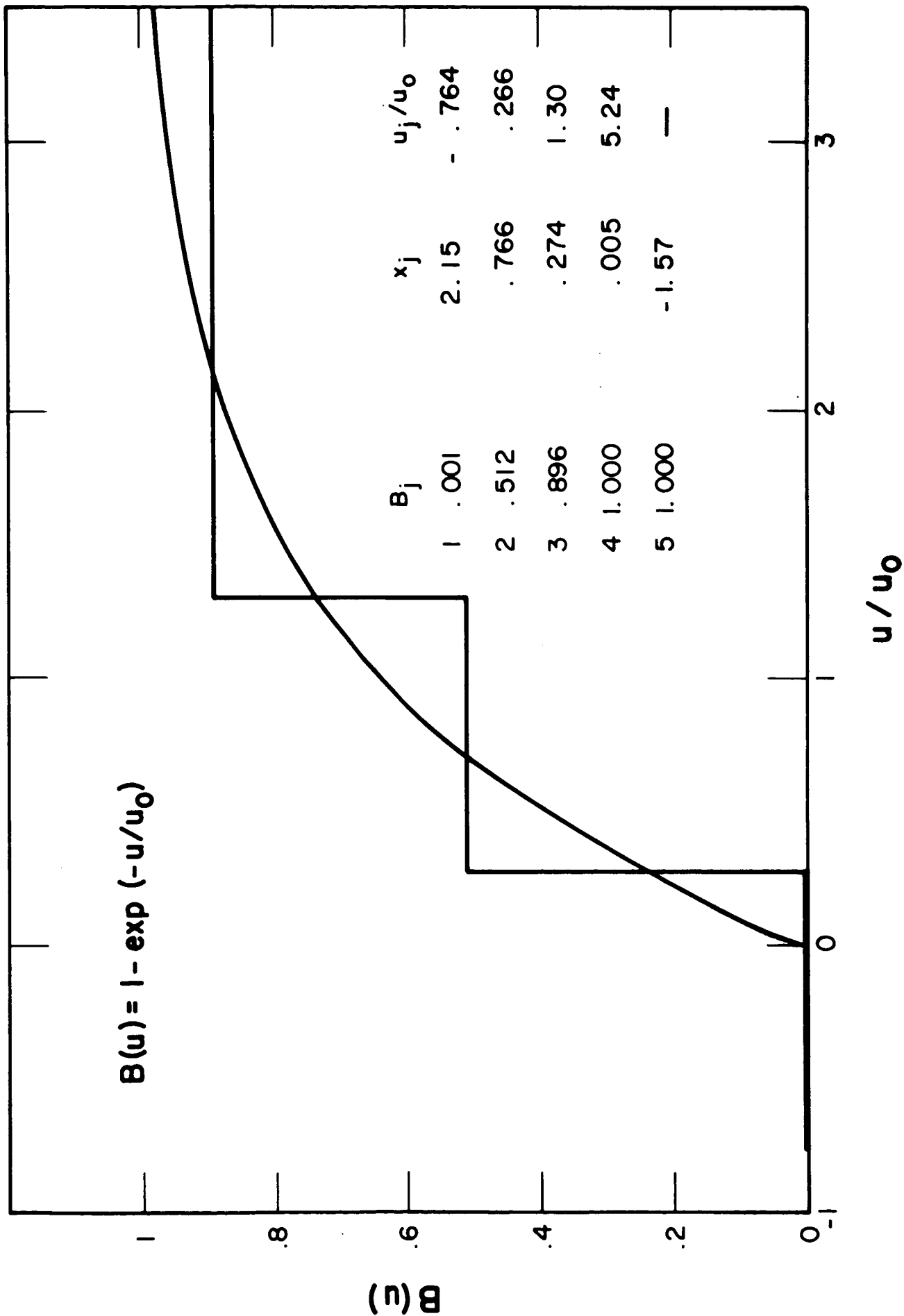


Figure 3. Inferred atmosphere with three-decimal observation accuracy.

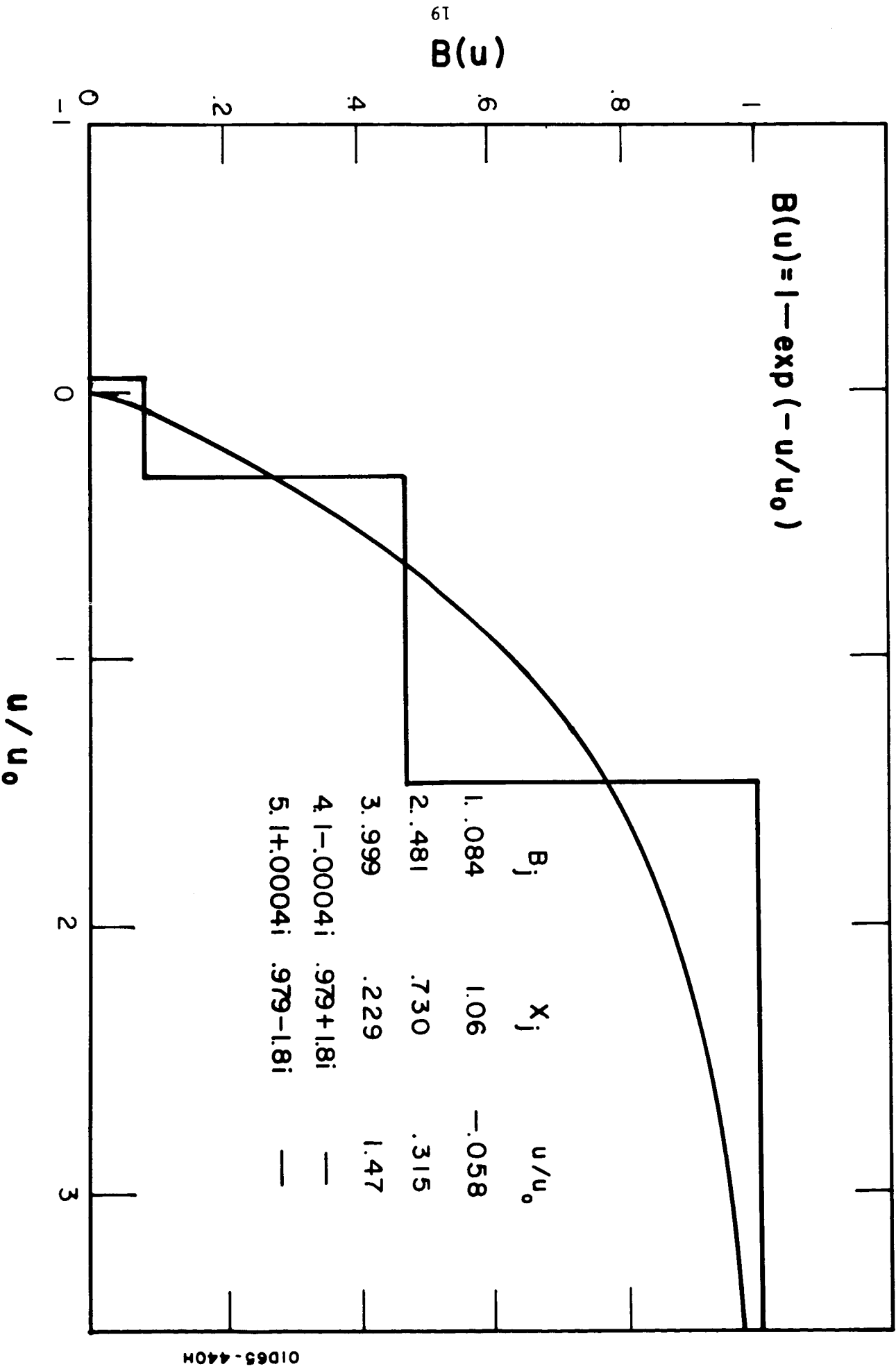


Figure 4. Inferred atmosphere with two-decimal observation accuracy.



APPENDIX A

MOMENT METHOD FOR SOLUTION OF THE  
SCHWARZSCHILD-MILNE INTEGRAL EQUATION

# MOMENT METHOD FOR SOLUTION OF THE SCHWARZSCHILD-MILNE INTEGRAL EQUATION

JEAN I. F. KING AND E. T. FLORANCE

Geophysics Corporation of America, Bedford, Massachusetts

Received July 18, 1963

## ABSTRACT

The underlying basis of the extreme accuracy of the double-Gauss quadrature formula devised in the method of discrete ordinates is uncovered in an alternative solution of the transfer equation. The Schwarzschild-Milne integral equation is solved by approximating the exponential integral kernel with a finite sum of exponential functions. A moment method is used to provide the best fit to the kernel. The constants that result are identical to those following from the choice of a double-Gauss quadrature formula in the discrete ordinate method. The integral equation formalism is then applied to the non-gray atmosphere problem.

## I. INTRODUCTION

The method of discrete ordinates developed by Wick (1943) and Chandrasekhar (1950) is a powerful technique for the solution of transfer equations. A critical factor is the choice of a proper quadrature formula to replace the integration of radiation intensity over direction. Sykes (1951) obtained results of extreme accuracy by splitting the interval and fitting the Gaussian formula separately over the upward and downward directions.

The physical basis for the success of the double-Gauss method is laid bare by an alternative solution of the equilibrium transfer-equation which does not involve the intensity. The Schwarzschild-Milne integral equation is approximately solved by expanding the kernel transmittance in a summation of exponential functions. The characteristic equation that results is formally identical with that of the method of discrete ordinates. The specification of a "best fit" of the kernel, and its approximate representation by equating moments, lead to a set of equations which reduce to the Legendre polynomials of the double-Gauss method. Thus the *ad hoc* choice of the double-Gauss formula is justified as providing the optimum fit of the exponential integral kernel by a finite sum of exponential functions.

## II. MOMENT-METHOD SOLUTION OF THE SCHWARZSCHILD-MILNE EQUATION

The transfer equation specifies a relation between the radiation intensity and Planck source function which, for a plane-parallel, non-scattering, gray atmosphere, may be written as

$$\mu \frac{dI(\tau, \mu)}{d\tau} = I(\tau, \mu) - B(\tau). \quad (1)$$

The imposition of the equilibrium constraint

$$B(\tau) = \frac{1}{2} \int_{-1}^1 I(\tau, \mu) d\mu \quad (2)$$

permits the elimination of either of these dependent variables. Thus, by substituting the source function (2) into equation (1) we obtain the equilibrium integrodifferential equation of transfer

$$\mu \frac{dI(\tau, \mu)}{d\tau} = I(\tau, \mu) - \frac{1}{2} \int_{-1}^1 I(\tau, \mu') d\mu'. \quad (3)$$

The method of discrete ordinates solves the problem approximately by converting the integrodifferential equation into a system of  $2n$  linear differential equations. This is done by replacing the integration over direction with a suitably chosen quadrature formula

$$\int_{-1}^1 I(\tau, \mu) d\mu \approx \sum_i a_i I(\tau, \mu_i) \quad (i = \pm 1, \dots, \pm n). \quad (4)$$

Chandrasekhar's (1950) use of a Gaussian quadrature formula was criticized by Kourganoff (1952) who preferred the Newton-Cotes method. Sykes (1951), meanwhile, obtained results of extreme accuracy by splitting the interval and fitting the Gaussian formula separately over the ranges  $(-1, 0)$  and  $(0, 1)$ . We now demonstrate the physical basis underlying Sykes's choice of a double-Gauss method, showing how it represents the optimum choice of a polynomial quadrature formula.

Returning to equations (1) and (2), we can use the equilibrium constraint alternatively to eliminate the intensity from the integral form of the transfer equation yielding (see Chandrasekhar [1950])

$$B(\tau) = \frac{1}{2} \int_{-\infty}^{\infty} B(t) E_1(|t - \tau|) dt, \quad (5)$$

the Schwarzschild-Milne integral equation. The direct solution of this equation is difficult. The form of the kernel

$$E_1(\tau) \equiv \int_0^1 e^{-\tau/\mu} \frac{d\mu}{\mu} \approx \sum_{i=1}^n \frac{a_i}{\mu_i} e^{-\tau/\mu_i} \quad (6)$$

suggests an approximate expansion into a summation of more tractable exponential functions.

Equation (5) becomes, with this kernel approximation,

$$B(\tau) = \frac{1}{2} \int_{-\infty}^{\infty} B(t) \sum_{i=1}^n \frac{a_i}{\mu_i} e^{-|t-\tau|/\mu_i} dt. \quad (7)$$

The application of the Laplace transform using the Faltung theorem (Sneddon [1951]) leads directly to

$$B(k) = \frac{1}{2} B(k) \sum_{i=1}^n \left( \frac{a_i}{1 + \mu_i k} + \frac{a_i}{1 - \mu_i k} \right), \quad (8)$$

where

$$B(k) \equiv \int_0^{\infty} B(\tau) e^{-k\tau} d\tau. \quad (9)$$

The requirement that  $B(k) \neq 0$  then yields as the *characteristic equation*

$$1 - \sum_{i=1}^n \frac{a_i}{1 - \mu_i^2 k^2} = 0, \quad (10)$$

whose  $2n - 1$  solutions consist of a double root at the origin  $k^2 = 0$  and paired roots at  $k = \pm k_a$ .

We obtain the general solution for the equilibrium source function by performing an inversion of equation (8) with the poles along the real axis given by the roots of the characteristic equation. Thus

$$B(\tau) = b \left[ \tau + Q + \sum_{a=1}^{n-1} (L_a e^{-k_a \tau} + L_{-a} e^{k_a \tau}) \right]. \quad (11)$$

The constants  $b$ ,  $Q$ ,  $L_a$ , and  $L_{-a}$  can be determined by boundary conditions in either of two ways. For a semi-infinite atmosphere the Wiener-Hopf technique can be used to express the constants directly as residues of the  $H$ -functions (King 1955), yielding

$$b = 3F/4, \quad Q = \sum_{i=1}^n \mu_i - \sum_{a=1}^{n-1} \frac{1}{k_a}, \tag{12}$$

$$L_a = \lim_{\mu \rightarrow 1/k_a} \frac{(1 - k_a \mu)}{\sqrt{3}} H(-\mu), \quad L_{-a} = 0,$$

where the  $H$ -function is given in this approximation as

$$H(\mu) = \frac{1}{\mu_1 \dots \mu_n} \frac{\prod_{i=1}^n (\mu + \mu_i)}{\prod_{a=1}^{n-1} (1 + k_a \mu)}. \tag{13}$$

Alternatively one can determine the constants by the requirement that  $B(\tau) = 0$  for  $\tau < 0$ . This constraint leads to a set of linear simultaneous equations to determine the  $n$  constants  $Q$ ,  $L_a$ . Upon using the method of elimination of constants we are led then to relations (12).

The characteristic equation (10) and constant relations (12) derived from the Schwarzschild-Milne equation are formally identical to those obtained by Chandrasekhar (1950) using the method of discrete ordinates. This is not surprising since the two approaches are transformations of the same problem.

The result is more than an elegant identity. First, we have derived the equilibrium source function  $B(\tau)$  directly without recourse to any auxiliary function such as the radiation intensity. More importantly, however, we have in the kernel approximation, equation (6), an algorithm for the specification of the best quadrature formula.

We return to the kernel approximation and determine the weights  $a_i$  and directions  $\mu_i$  by equating moments of the kernel with its series approximation. Thus

$$\int_0^\infty E_1(\tau) \tau^l d\tau = \sum_{i=1}^n \frac{a_i}{\mu_i} \int_0^\infty e^{-\tau/\mu_i} \tau^l d\tau, \tag{14}$$

yielding the following system of non-linear equations to determine the  $2n$  constants  $a_1, \dots, a_n$  and  $\mu_1, \dots, \mu_n$

$$\sum_{i=1}^n a_i \mu_i^l = E_{l+2}(0) = \frac{1}{l+1} \quad (l = 0, 1, \dots, 2n - 1). \tag{15}$$

### III. SOLUTION OF MOMENT EQUATIONS

A method for solving moment equations of the type

$$\sum_{i=1}^n a_i \mu_i^l = b_l \quad (l = 0, \dots, 2n - 1) \tag{16}$$

has been given by Chandrasekhar (1950). He shows that if coefficients  $c_j$  ( $j = 0, \dots, n - 1$ ) are defined by the linear equations

$$b_{n+l} + \sum_{j=0}^{n-1} c_j b_{j+l} = 0 \quad (l = 0, \dots, n - 1), \tag{17}$$

then  $\mu_i$  is one of the  $n$  roots of the polynomial

$$F(x) \equiv x^n + \sum_{j=0}^{n-1} c_j x^j. \quad (18)$$

The coefficients  $c_j$  can be eliminated from equations (17) and (18), with the result that  $F(x)$  is a multiple of the polynomial

$$\Phi(x) \equiv \det [\hat{b}_{jl}(x)], \quad (19)$$

where  $\hat{b}(x)$  is the  $(n+1) \times (n+1)$  matrix

$$\hat{b}_{jl} = b_{j+l} \quad (j = 0, \dots, n-1), \quad \hat{b}_{nl} = x^l \quad (l = 0, \dots, n). \quad (20)$$

The determinantal equation  $\Phi(x) = 0$  in which we have from equation (15)

$$b_l = \frac{1}{l+1} = \int_0^1 x^l dx \quad (21)$$

can be simplified (Muir 1960) to the form

$$\frac{d^n}{dx^n} [x^n (1-x)^n] = 0. \quad (22)$$

The substitution

$$x = \frac{1}{2}(1 + \bar{x}) \quad (23)$$

immediately reduces equation (22) to the equation

$$P_n(\bar{x}) = 0,$$

where  $P_n$  is the Legendre polynomial of order  $n$ . Thus, we have arrived at the same result as the Sykes double-Gauss method:

$$\mu_i = \frac{1}{2}(1 + \bar{\mu}_i), \quad (24)$$

where  $\bar{\mu}_i$  is one of the  $n$  roots of the Legendre polynomial  $P_n$ .

Since the transformation (23) maps the interval  $(-1, 1)$  onto  $(0, 1)$ , Sykes (1951) noted that the double-Gauss formula is merely the Gaussian formula applied to the transformed interval. We will now demonstrate that the linear mapping (23) correctly transforms the moment equations (16).

If we insert equation (23) into the definition

$$b_l = \int_{-1}^1 \bar{x}^l d\bar{x}$$

and use the moment equations (16) with equation (24), we obtain the transformed equations

$$\sum_{i=1}^n \bar{a}_i \bar{\mu}_i^l = b_l, \quad (25)$$

where  $\bar{a}_i = 2a_i$ . In other words, a solution to the equations (16) for the interval  $(0, 1)$  is a linear function of the solution to equation (25) on the interval  $(-1, 1)$ .

The solution to equation (25) with

$$\bar{b}_l = 0 \quad (l \text{ odd}), \quad \bar{b}_l = \frac{2}{l+1} \quad (l \text{ even}),$$

is the familiar Gaussian formula (Chandrasekhar 1950). Hence, the weights  $a_i$  are given by

$$a_i = \frac{1}{2} \frac{1}{P_n'(\bar{\mu}_i)} \int_{-1}^1 d\bar{\mu} \frac{P_n(\bar{\mu})}{\bar{\mu} - \bar{\mu}_i} \tag{26}$$

Writing equation (26) in the form

$$a_i = \left[ \frac{dP_n}{d\mu_i}(2\mu_i - 1) \right]^{-1} \int_0^1 d\mu \frac{P_n(2\mu - 1)}{\mu - \mu_i}$$

reveals the standard prescription of  $a_i$  as a quadrature weight.

TABLE 1  
CHARACTERISTIC ROOTS AND CONSTANTS OF INTEGRATION

Approximation	Direction Cosine	Characteristic Roots	Q-Constant	L-Constants
First.....	$\mu_1 = 0.50000000$		+0.500000	
Second.....	$\mu_1 = .21132487$ $\mu_2 = .78867513$	$k_1 = 3.46410162$	+ .711325	$L_1 = -0.133975$
Third.....	$\mu_1 = .11270167$ $\mu_2 = .50000000$ $\mu_3 = .88729834$	$k_1 = 1.52028083$ $k_2 = 7.59531080$	+ .710567	$L_1 = - .057038$ $L_2 = - .076179$
Fourth.....	$\mu_1 = .06943184$ $\mu_2 = .33000948$ $\mu_3 = .66999052$ $\mu_4 = 0.93056816$	$k_1 = 13.12234030$ $k_2 = 1.22721388$ $k_3 = 2.50960776$	+0.710472	$L_1 = - .048082$ $L_2 = - .024173$ $L_3 = -0.060866$

TABLE 2  
COMPARISON OF FOURTH APPROXIMATION AND EXACT SOLUTIONS

$\tau$	$q_{ap}(\tau)$	$p_{ex}(\tau)$	$\mu$	$H_{ap}(\mu)$	$H_{ex}(\mu)$
0.00.....	0.57735	0.577351	0.0	1.00000	1.0000000
0.01.....	.58507	.588236	0.1	1.24619	1.2473502
0.02.....	.59202	.595391	0.2	1.45020	1.4503515
0.04.....	.60396	.606287	0.3	1.64257	1.6425221
0.06.....	.61378	.614789	0.4	1.82937	1.8292757
0.08.....	.62194	.621854	0.5	2.01288	2.0127788
0.10.....	.62879	.627919	0.6	2.19423	2.1941330
0.20.....	.65123	.649550	0.7	2.37407	2.3739750
0.40.....	.67312	.673090	0.8	2.55279	2.5527044
0.60.....	.68537	.685801	0.9	2.73067	2.7305876
0.80.....	.69324	.693535	1.0	2.90789	2.9078105
1.00.....	.69844	.698540			
2.00.....	.70799	.707916			
3.00.....	.70983	.709806			
$\infty$ .....	0.71047	0.710447			

The characteristic equation (10) has been solved up to the fourth approximation. The roots  $\mu_i$  and  $k_a$  along with the derived constants  $Q$  and  $L_a$  from equation (12) are given for reference in Table 1. As an indication of the superior accuracy of the double-Gauss method, in Table 2 we compare the fourth approximation for  $q(\tau)$  and  $H(\mu)$  with the exact result from Kourganoff (1952, p. 138, Tables 33, 34).

## IV. EXTENSION TO NON-GRAY ATMOSPHERES

The Schwarzschild-Milne integral equation approach shows to best advantage in an extension to the non-gray atmosphere problem. The flux transmittance for a narrow band of width  $\Delta\nu$  consisting of many lines, yet small enough so that the Planck function is sensibly constant, is defined as

$$\begin{aligned} 2\mathcal{E}_3(\tau) &= \frac{2}{\Delta\nu} \int_{\Delta\nu} \int_0^1 e^{-\kappa_\nu \nu/\mu} \mu \, d\mu \, d\nu \\ &= 2 \int_0^1 \int_0^1 e^{-\tau/\mu\lambda} \mu \, d\mu \, d(\nu/\Delta\nu), \end{aligned} \quad (27)$$

where  $\lambda = \kappa/\kappa_\nu$  is the ratio of the arithmetic mean and monochromatic absorption coefficients.

By analogy with the gray case we can define a hierarchy of non-gray transmittances by

$$\mathcal{E}_n(\tau) = \int_0^1 \int_0^1 e^{-\tau/\mu\lambda} (\mu\lambda)^{n-2} d\mu \frac{d(\nu/\Delta\nu)}{\lambda}, \quad (28)$$

obeying the relation

$$\frac{d\mathcal{E}_n(\tau)}{d\tau} = -\mathcal{E}_{n-1}(\tau) \quad (n = 2, 3, \dots). \quad (29)$$

The non-gray Schwarzschild-Milne equation becomes

$$B(\tau) = \frac{1}{2} \int_{-\infty}^{\infty} B(t) \mathcal{E}_1(|t - \tau|) dt. \quad (30)$$

As we continue to exploit the analogy, the form of the equation suggests that we expand the kernel in a summation of exponential functions

$$\mathcal{E}_1(\tau) \approx \sum_{i=1}^n \frac{a_i}{\mu_i} e^{-\tau/\mu_i}, \quad (31)$$

where the  $a_i$  and  $\mu_i$  are now "generalized" weights and roots.

Equating moments as before, these constants are determined by the system of  $2n$  non-linear simultaneous equations

$$\sum_{i=1}^n a_i \mu_i^l = \mathcal{E}_{l+2}(0) \equiv \beta_l \quad (l = 0, 1, \dots, 2n - 1). \quad (32)$$

Thus the non-gray problem is reduced simply to the determination of new constants specified by different moments. Using relation (27) we may tabulate these as

$$\begin{aligned} \mathcal{E}_2(0) &= 1, \mathcal{E}_3(0) = \frac{1}{2}, \mathcal{E}_4(0) = \langle \lambda \rangle / 3, \mathcal{E}_5(0) = \langle \lambda^2 \rangle / 4, \dots, \\ \mathcal{E}_n(0) &= \langle \lambda^{n-3} \rangle / (n - 1). \end{aligned} \quad (33)$$

As an example consider an Elsasser band model consisting of an equally spaced array of identical Lorentz lines whose monochromatic absorption coefficient is

$$\kappa_\nu = \frac{S}{d} \frac{\sinh(2\pi\alpha/d)}{\cosh(2\pi\alpha/d) - \cos(2\pi\nu/d)}, \quad (34)$$

where  $S$ ,  $a$ , and  $d$  are the line intensity, half-width, and spacing. By integrating from line center to center we obtain the relations

$$\kappa = \frac{S}{d}, \langle \lambda \rangle = \frac{\kappa}{\kappa_h} = \coth \beta, \quad \langle \lambda^2 \rangle = \frac{\frac{1}{2} + \cosh^2 \beta}{\sinh^2 \beta}, \quad (35)$$

where  $\langle \lambda \rangle$ , the non-grayness parameter, is the ratio of the arithmetic and harmonic means of the absorption coefficient and  $\beta = 2\pi a/d$  is the ratio of line half-width and spacing. Any deviation from grayness leads to a  $\langle \lambda \rangle$  in excess of unity.

Although the  $\mu_i$  in equation (32) are no longer roots of the Legendre polynomials as in the gray case, it is not difficult to solve the equation set explicitly in the  $n = 2$  approximation. Doing this we find  $\mu_1, \mu_2$  as roots of the quadratic equation

$$(\beta_0\beta_2 - \beta_1^2)\mu^2 - (\beta_0\beta_3 - \beta_1\beta_2)\mu + (\beta_1\beta_3 - \beta_2^2) = 0, \quad (36)$$

with the root of the characteristic equation given by

$$k_1 = \sqrt{\left(\frac{\beta_2}{\beta_0}\right) \frac{\beta_0\beta_2 - \beta_1^2}{\beta_1\beta_3 - \beta_2^2}}. \quad (37)$$

The most interesting result, identical in all orders of approximation and hence exact, is the Hopf-Bronstein relation generalized now for a non-gray atmosphere. Thus

$$q(0) \equiv Q + L_1 = \mu_1\mu_2k = \sqrt{(\beta_2/\beta_0)} = \sqrt{\langle \lambda \rangle / 3}. \quad (38)$$

The remaining constants in this approximation are determined as

$$Q = \mu_1 + \mu_2 - \frac{1}{k_1} = \frac{\beta_0\beta_3 - \beta_1\beta_2 - (\beta_0/\beta_2)^{1/2}(\beta_1\beta_3 - \beta_2^2)}{\beta_0\beta_2 - \beta_1^2}, \quad (39)$$

$$L_1 = \sqrt{(\beta_2/\beta_0)} - Q.$$

#### V. CONCLUSIONS

The double-Gauss quadrature formula used by Sykes (1951) has a sound physical basis in providing the optimum fit of the kernel in the Schwarzschild-Milne integral equation by an exponential function series. The power of the alternative integral equation formulation is demonstrated by the ease in the extension to treat non-gray atmospheres.

We are grateful to Robert V. Sillars for the calculations leading to Tables 1 and 2. The research reported in this paper has in part been supported by the National Aeronautics and Space Administration under contract NAS5-3352.

#### REFERENCES

- Chandrasekhar, S. 1950, *Radiative Transfer* (Oxford: Clarendon Press).  
 King, J. I. F. 1955, *Guenther Laeser Memorial Lecture*, GRD-TN-60-603, Geophysics Research Directorate, AF Cambridge Research Laboratories, Bedford, Massachusetts.  
 Kourganoff, V. 1952, *Basic Methods in Transfer Problems* (Oxford: Clarendon Press).  
 Muir, T. 1960, *Treatise on the Theory of Determinants* (New York: Dover Publications).  
 Sneddon, I. N. 1951, *Fourier Transforms* (New York: McGraw-Hill Book Co.).  
 Sykes, J. B. 1951, *M.N.*, 111, 377.  
 Wick, G. C. 1943, *Zs. f. Phys.*, 120, 702.



APPENDIX B

GREENHOUSE EFFECT IN A SEMI-INFINITE ATMOSPHERE

## Greenhouse Effect in a Semi-Infinite Atmosphere

JEAN I. F. KING

*Geophysics Corporation of America, Bedford, Massachusetts*

Communicated by Z. Sekera

Received September 23, 1963

A formalism is developed for solving the radiative transfer equation in the presence of imbedded heat sources. This is accomplished by demonstrating the equivalence of an internally heated model atmosphere to the well-known problem of diffuse reflection from an isotropically scattering atmosphere. A replacement algorithm is then used to calculate the steady state limb-darkening and vertical thermal profile of a semi-infinite, plane-parallel atmosphere heated solely from above. In our model the heat source, due to direct absorption of sunlight, is a maximum at the top of the atmosphere and falls off exponentially with increasing depth.

The greenhouse factor, defined as the ratio of the Planck temperature for large depth and the effective temperature of an externally viewed planet, is found as  $[B(\infty)/B_{eff}] = \sqrt{3}H(\mu_0)/4$ , where  $\mu_0$  is the ratio of infrared and visible absorption coefficients.  $H(\mu_0)$  is the Chandrasekhar  $H$  function, generalized for values of the argument  $\mu_0$  greater than unity. The strong dependence of the greenhouse effect on the ratio of absorption coefficients at differing spectral regions is expected. It comes as an intuitive surprise, however, to note that a pure gray atmosphere [ $\mu_0 = 1$ ,  $H(\mu_0) = 2.9078$ ] whose heating is concentrated at the upper levels nonetheless exhibits limb-darkening and steady state increase of temperature with depth.

### INTRODUCTION

The greenhouse effect which occurs in externally heated planetary atmospheres is qualitatively well understood. The phenomenon, which results in a temperature enhancement near the surface, derives from the valving action of the atmosphere in admitting the solar flux at optical wavelengths while trapping the re-emitted radiation in the far infrared. Clearly this effect must depend fundamentally on the contrast between atmospheric visual transparency and infrared opacity.

The heating due to the incoming solar beam as it attenuates in the atmosphere plays a central role. In a steady state configuration the temperature must accommodate to this flux so that the loss through infrared emission exactly balances the energy gain from solar absorption. We seek, therefore, a formalism which will yield the steady state temperature profile for an internal

heat source of suitably chosen configuration. This goal is obtained obliquely by relating the imbedded source model to the well-known problem of the diffuse reflection from a scattering atmosphere.

### THEORY

We begin by integrating the transfer equation for a plane-parallel absorbing atmosphere,

$$\mu[dI(\tau, \mu)/d\tau] = I(\tau, \mu) - B(\tau), \quad (1)$$

over all directions yielding the flux divergence

$$\frac{1}{4}[dF(\tau)/d\tau] = \frac{1}{2} \int_{-1}^1 I(\tau, \mu) d\mu - B(\tau). \quad (2)$$

Under radiative equilibrium the flux divergence must vanish. In our problem, on the other hand, this term which is proportional to the infrared heating must remain finite.

centrated at infinite depths. Using Eq. (10) the upwelling intensity for such a source becomes

$$\lim_{\mu_0 \rightarrow \infty} I(0, \mu) = \sqrt{3}(F/4)H(\mu), \quad (11)$$

a result identical to the emerging intensity from a semi-infinite atmosphere in radiative equilibrium.

Figure 1 displays limb-darkening curves

welling radiation from a semi-infinite atmosphere is the Laplace transform of the source function. Thus

$$I(0, \mu) = \int_0^\infty B(\tau) \exp(-\tau/\mu) d\tau/\mu = \mathbf{B}(1/\mu)/\mu, \quad (12)$$

where

$$\mathbf{B}(p) \equiv \int_0^\infty B(\tau) \exp(-p\tau) d\tau. \quad (13)$$

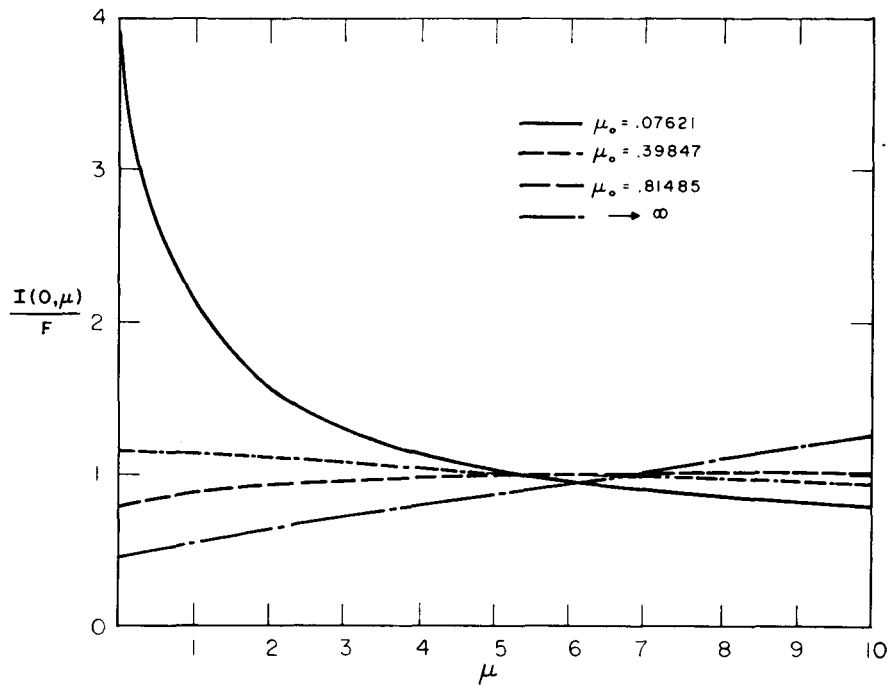


FIG. 1. Limb-darkening for various attenuated sources  $(F/4\mu_0) \exp(-\tau/\mu_0)$ .

for imbedded exponential sources of various scale lengths. The shorter the scale length  $\mu_0$ , the more concentrated the source at the top of the atmosphere. As expected the curves for small  $\mu_0$  exhibit limb-brightening. Of surprise, however, is the fact that already for  $\mu_0 = 0.815$ , limb-darkening is becoming apparent. Limb-darkening becomes most pronounced in the greenhouse "limit" as the atmosphere becomes transparent in the visible, corresponding to  $\mu_0$  approaching infinity.

In order to obtain  $B(\tau)$  for various heating configurations we use the fact that the up-

The source function follows from Eq. (8) as the inverse transform

$$B(\tau) = \frac{1}{2\pi i} \frac{F}{4} \frac{H(\mu_0)}{\mu_0} \int_{\gamma-i\infty}^{\gamma+i\infty} \frac{H(p)}{p + (1/\mu_0)} \exp(p\tau) dp. \quad (14)$$

Using the quotient polynomial expression (9) for the  $H$  function, we have as the contour integral

$$B(\tau) = \frac{1}{2\pi i} \frac{F}{4} \frac{H(\mu_0)}{\mu_0 \mu_1 \dots \mu_n}$$

Elimination of the source function  $B(\tau)$  from Eqs. (1) and (2) results in

$$\mu[dI(\tau, \mu)/d\tau] = I(\tau, \mu) - \frac{1}{2} \int_{-1}^1 I(\tau, \mu') d\mu' + \frac{1}{4}[dF(\tau)/d\tau], \quad (3)$$

which is to be compared with the transfer equation for the problem of diffuse reflection by an atmosphere scattering radiation isotropically (Chandrasekhar, 1950, p. 81)

$$\mu[dI(\tau, \mu)/d\tau] = I(\tau, \mu) - \frac{1}{2} \int_{-1}^1 I(\tau, \mu') d\mu' - (F/4) \exp(-\tau/\mu_0). \quad (4)$$

Except for the inhomogeneous terms the equations are identical. This formal similarity implies that the intensity and source function for an atmosphere diffusely reflecting a parallel beam incident downward in the direction  $-\mu_0$ , are proportional to  $I(\tau, \mu)$  and  $B(\tau)$  for a model atmosphere with an internal heat sink given by

$$\frac{1}{4}[dF(\tau)/d\tau] = -(F/4\mu_0) \exp(-\tau/\mu_0), \quad (5)$$

where the normalization factor  $1/\mu_0$  guarantees that  $F(\tau \rightarrow \infty) = 0$ .

Under steady state the infrared loss must be exactly compensated by a matching gain from the absorbed solar beam. If we assume a monochromatic beam for simplicity, we have

$$-\frac{1}{4} \frac{dF}{d\tau} \Big|_{ir} = \frac{1}{4} \frac{dF}{d\tau} \Big|_{vis} = \frac{F(0)}{4\mu_0} \exp(-\kappa_{vis}u), \quad (6)$$

where  $\kappa_{vis}$  is the absorption coefficient of the solar beam. On comparing Eqs. (5) and (6) remembering the definition,  $\tau = \kappa_{ir}u$ , we are led to associate  $\mu_0$  with the ratio of absorption coefficients,

$$\mu_0 = \kappa_{ir}/\kappa_{vis}. \quad (7)$$

Thus we have proved the following lemma:

*The intensity and source function for a steady state atmosphere being heated by a nonthermal source whose flux divergence is given by  $[F(0)/4\mu_0] \exp(-\tau/\mu_0)$  is equivalent to  $I(\tau, \mu)$  and  $B(\tau)$  for an atmosphere diffusely reflecting a parallel beam of strength  $F/4\mu_0$ . The solutions are identical. From an examination of the intensity or source function alone it is impossible to discern whether*

the radiation arises from an externally imposed flux or an internally supplied source of nonthermal origin. This interchangeability of internal and external constraints has far-reaching implications for the solution of a variety of radiative transfer problems.

The imbedded source problem admits a generalization denied the impressed beam model in which the direction cosine  $\mu_0$  is restricted to the range zero to one. In the imbedded source analog  $\mu_0$  as defined by Eq. (7) can take any positive value and, in greenhouse models, typically greatly exceeds unity. As we shall see this leads to a natural generalization of the  $H(\mu)$  function for argument greater than one.

Having demonstrated the equivalence of the two models, we can appropriate directly some of the results of the diffuse reflection problem. Using the replacement algorithm [Eq. (5)] we find for an atmosphere heated internally by a exponential source  $(F/4\mu_0) \exp(-\tau/\mu_0)$ , that the upwelling radiation is given by

$$I(0, \mu) = \frac{F}{4} \frac{H(\mu)H(\mu_0)}{\mu + \mu_0}. \quad (8)$$

There is no mathematical difficulty involved in generalizing the  $H$  function for argument greater than unity. For suitably chosen constants (King and Florance, 1964) the quotient polynomial form

$$H(\mu) = \frac{1}{\mu_1 \dots \mu_n} \frac{\prod_{i=1}^n (\mu_i + \mu)}{\prod_{\alpha=1}^n (1 + k_{\alpha}\mu)}, \quad (9)$$

is convenient, yielding even for  $n = 4$  an approximation of extreme accuracy. Further, it follows readily that

$$\lim_{\mu \rightarrow \infty} \frac{1}{\mu} H(\mu) = \frac{1}{\mu_1 \dots \mu_n k_1 \dots k_{n-1}} = \sqrt[n]{3} \quad (10)$$

a result valid for all orders of approximation and hence exact.

Thus we see that as  $\mu_0 \rightarrow \infty$ , the imbedded source approaches zero for finite values of the optical depth  $\tau$ , with the heating con-

$$\int_{\gamma-i\infty}^{\gamma+i\infty} \frac{\exp p\tau}{p + (1/\mu_0)} \frac{\prod_{i=1}^n (\mu_i p + 1)}{p \prod_{\alpha=1}^n (p + k_\alpha)} dp, \quad (15)$$

which has  $n + 1$  simple poles at  $p = 0$ ,  $-k_\alpha$ , and  $-1/\mu_0$ .

A straightforward evaluation yields

$$B(\tau) = \sqrt{3} \frac{F}{4} H(\mu_0) \left[ 1 + \sum_{\alpha=1}^{n-1} \frac{k_\alpha L_\alpha \exp(-k_\alpha \tau)}{k_\alpha \mu_0 - 1} + \frac{H(-\mu_0) \exp(-\tau/\mu_0)}{\sqrt{3} \mu_0} \right], \quad (16)$$

with

$$L_\alpha \equiv (-1)^n k_1 \dots k_{n-1} \frac{\prod_{i=1}^n [(1/k_\alpha) - \mu_i]}{\prod_{\beta=1}^{n-1} [1 - (k_\beta/k_\alpha)]} \quad (17)$$

where the prime denotes the factor  $\beta = \alpha$  is omitted.

We note that as  $\mu_0$  approaches infinity, we have, using L'Hospital's rule

$$\lim_{\mu_0 \rightarrow \infty} B(\tau) = 3 \frac{F}{4} \left[ \sum_{\alpha=1}^{n-1} L_\alpha \exp(-k_\alpha \tau) + \tau + Q \right], \quad (18)$$

where

$$Q = \sum_{i=1}^n \mu_i - \sum_{\alpha=1}^{n-1} 1/k_\alpha. \quad (19)$$

Thus we reclaim the familiar radiative equilibrium result.

Care must be exercised in the evaluation of  $B(\tau)$  for imbedded sources whose scale factors coincide with reciprocal roots of the characteristic equation, i.e. for cases in which  $\mu_0 = 1/k_\alpha$ . In this event we see, using the quotient form of  $H(-\mu_0)$  defined by relation (9), that the final two terms of the source

function, Eq. (16), separately diverge. An application of L'Hospital's rule shows that their sum, however, yields a finite residue leading, for  $\mu_0 = 1/k_\alpha$  to,

$$B(\tau) = \sqrt{3} \frac{F}{4} k_\alpha H\left(\frac{1}{k_\alpha}\right) \left[ \frac{1}{k_\alpha} + \sum_{\beta=1}^{n-1} \frac{k_\beta L_\beta \exp(-k_\beta \tau) + k_\alpha L_\alpha \exp(-k_\alpha \tau)}{k_\beta - k_\alpha} - k_\alpha L_\alpha \exp(-k_\alpha \tau) \left( \tau + \sum_{i=1}^n \frac{\mu_i}{1 - k_\alpha \mu_i} + \frac{1}{k_\alpha} \right) \right]. \quad (20)$$

This is to be expected since there is no reason to attach special physical significance to the values  $\mu_0 = 1/k_\alpha$ .

The ratio of the source function at large depths to that at the surface is easily found. From Eq. (16) we have

$$B(\tau \rightarrow \infty) = \sqrt{3}(F/4)H(\mu_0). \quad (21)$$

At the top of the atmosphere we find from Eq. (8)

$$B(0) = I(0,0) = (F/4)[H(\mu_0) \mu_0], \quad (22)$$

yielding as our ratio

$$B(\infty)/B(0) = \sqrt{3} \mu_0. \quad (23)$$

a result known to Chandrasekhar (1950, p. 87), though interpretable now for arbitrary value of  $\mu_0$ .

If we so chose, the greenhouse factor could be defined as this ratio of source functions. A more physically satisfying definition, however, is the ratio of  $B(\infty)$  to the effective black-body function of the outgoing flux, which yields the surface temperature of an equivalent atmosphereless planet. From the definition it follows that  $B_{eff} = F$ , since

$$F/4 = \frac{1}{2} \int_0^1 I(0,\mu) \mu d\mu = \frac{1}{2} \int_0^1 B_{eff} \mu d\mu = B_{eff}/4. \quad (24)$$

The greenhouse factor, which represents the temperature enhancement due to the presence of an atmosphere, becomes, on using Eqs. (21) and (24)

$$B(\infty)/B_{eff} = (\sqrt{3} \cdot 4)H(\mu_0). \quad (25)$$

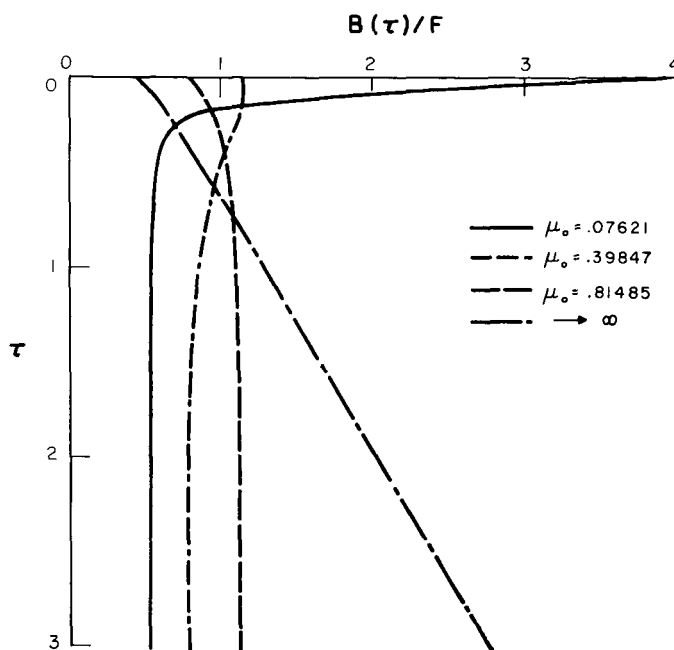


FIG. 2. Steady state Planck temperature profiles for various attenuated sources.

One customarily associates the greenhouse effect with models having a large infrared to visible absorption coefficient ratio [ $\mu_0 = (\kappa_{ir}/\kappa_{vis}) \gg 1$ ]. We see surprisingly that even for a "gray" atmosphere, Eq. (25)

$$B(\infty)/B_{eff} = (\sqrt{3}/4)H(\mu_0 = 1) = 1.259,$$

exceeds unity, indicating a greenhouse effect. Thus even in an atmosphere in which the heating is a maximum at the top, decreasing exponentially with depth, one may nonetheless have a greenhouse increase of temperature with depth and limb-darkening under steady state conditions. It is possible, therefore, for the atmosphere at large depths to have a higher temperature than overlying layers even though there is negligible penetration of sunlight to the depth in question.

Figure 2 is a plot of the source function

[Eq. (20)] for three models in which the absorption scale length  $\mu_0 = 1/k_\alpha$ , and a fourth curve for the equilibrium case,  $\mu_0 \gg 1$ . The general pattern emerging is that for concentrated sources,  $\mu_0 < (1/\sqrt{3})$ , the steady state temperature decreases with depth while sunlight which attenuates less rapidly leads to a greenhouse downward temperature increase.

#### ACKNOWLEDGMENT

This work has been supported in part by the National Aeronautics and Space Administration under Contract No. NAS5-3352.

#### REFERENCES

- CHANDRASEKHAR, S. (1950). "Radiative Transfer." Oxford Univ. Press, London.  
 KING, J. I. F., AND FLORANCE, E. T. (1964). *Astrophys. J.* In press.

APPENDIX C

RADIATIVE TRANSFER WITH IMBEDDED SOURCES

## APPENDIX C

### RADIATIVE TRANSFER WITH IMBEDDED SOURCES

#### I. Abstract

#### II. Introduction

A. Problem treated: Steady-state distribution of radiation in a plane-parallel, semi-infinite planetary atmosphere for arbitrary imbedded heat sources and sinks. Wanted: Vertical distribution of temperature and intensity profile of the upwelling radiation with viewing angle for various imbedded sources.

B. Relation between imbedded sources and boundary conditions.

C. Development of the fundamental Schwarzschild-Milne integral equation.

#### III. Wiener-Hopf Solutions of the Schwarzschild-Milne equation

##### A. Exponential type imbedded sources

1. 
$$S_+(\tau) = \frac{1}{\mu_0} \exp\left(\frac{-\tau/\mu_0}{\mu_0}\right), \mu_0 \text{ real}$$

a. relation to Chandrasekhar scattering problem for

$$\mu_0 < 1$$



- b. relation to radiative equilibrium model for  $\mu_0 \gg 1$   
 $\langle \text{deep imbedded source} \rangle$
- c. limiting cases given by  $S_+(\tau) = \delta(\tau)$  with  $\tau \rightarrow 0, \gg 1$
- d. simple greenhouse model interpreting  $\mu_0 = \kappa_{\text{ir}} / \kappa_{\text{vis}}$
- e. minimum free air temperature theorem
- f. plots of  $I(0, \mu), B(\tau)$  for various  $\mu_0$

2. 
$$S_+(\tau) = \frac{1}{\mu_0} \exp\left(\frac{-\tau/\mu_0}{\mu_0}\right), \mu_0 \text{ complex}$$

- a. generalization of H-function for complex argument
- b. physical interpretation: damped sinusoidal sources
- c. formulas for computing  $H(\mu_0), \mu_0 \text{ complex}$
- d. tables
- e. graphs

3. 
$$S_+(\tau) = \sum_{n=1}^m \frac{p(a_n)}{q'(a_n)} \exp(a_n \tau), \exp(a\tau) \sum_{n=1}^r \frac{p(r-n)(a)}{(r-n)!} \frac{\tau^{n-1}}{(n-1)!}$$

- a. Heaviside type expansion theorem for  $I(0, \mu)$
- b. application to expansion of  $S_+(\tau)$  in orthogonal polynomial sets

B. Exponential integral imbedded sources

1. 
$$S_+(\tau) = E_1(\tau)$$

- a. derivation of  $I_1(0, \mu), B_1(\tau)$
- b. equivalent boundary constraint

2. 
$$S_+(\tau) = 2 E_2(\tau)$$

- a. derivation of  $I_2(0, \mu) = B_2(\tau) = F \langle \text{isothermal case} \rangle$

b. equivalent boundary constraint

3. 
$$S_+(\tau) = n E_n(\tau)$$

a. derivation of  $I_n(0, \mu)$  for arbitrary integral  $n$

b. solutions  $I_3(0, \mu)$ ,  $I_4(0, \mu)$ ,  $B_3(\tau)$ ,  $B_4(\tau)$

C. Delta-function imbedded source: The Green's Function

1. Wiener-Hopf derivation of  $I(0, \mu)$ ,  $B(\tau) = G(\tau/\tau_1)$  for

$$S_+(\tau) = \delta(\tau - \tau_1).$$

2. Plots of  $I(0, \mu)$ ,  $B(\tau)$  for various  $\tau_1$ .

3. Improved greenhouse model.

4. Functional integral equation obeyed by Green's function.

5. Central role of H-function.

IV. Non-linear H-function integral equations derived using imbedded sources.

1. Relation to invariance principle.

2. H-function moments.

3. Alternative method for obtaining H-functions

$\langle$ moment method of K & F $\rangle$ .

V. Conclusions

1. Capability for general greenhouse models.

2. Generalization for non-gray atmospheres.

3. Implications for inversion problem.

4. Finite atmosphere.

APPENDIX D

INVERSION BY SLABS OF VARYING THICKNESS

## Inversion by Slabs of Varying Thickness

JEAN I. F. KING

*Geophysics Corporation of America, Bedford, Mass.*

26 March 1964

In the inversion problem an algorithm is sought for the inference of atmospheric vertical thermal structure from remotely-sensed radiometric observations. To accomplish this we propose a new inversion method, the variable slab technique, and demonstrate its application by two illustrative examples.

All inversion procedures attempt to recover the thermal profile from observations of the upwelling intensity  $I(\kappa/\mu)$  at various directions and/or frequencies. Transfer theory specifies the temperature dependence on depth as the solution of a linear integral equation

$$I(\kappa/\mu) = - \int_0^\infty B(u) \frac{\partial \mathfrak{K}}{\partial u} du, \quad (1)$$

where  $B$  is the Planck intensity considered here an implicit function of absorber depth  $u$ , and  $\mathfrak{K}$  is the kernel transmittance averaged over a narrow frequency interval

$$\mathfrak{K}(\kappa u/\mu) = \frac{1}{\Delta\nu} \int_{\Delta\nu} e^{-\kappa\nu u/\mu} d\nu, \quad (2)$$

with  $\kappa$ , the monochromatic absorption coefficient.

For our purposes a simplified gray, plane-parallel, fixed-frequency model suffices in which the intensity is scanned over nadir angle  $\theta = \cos^{-1}\mu$ . Under these conditions the intensity is a Laplace transform of the indicial function

$$I(1/\mu) = \int_0^\infty B(\tau) e^{-\tau/\mu} d\tau / \mu = \frac{b(1/\mu)}{\mu}, \quad (3)$$

where we have transformed to the new variable, optical depth  $\tau = \kappa u$ .

Conventionally the temperature profile is approximated by an appropriate series expansion

$$B(\tau) = \sum a_j F_j(\tau). \quad (4)$$

The series need not be orthogonal but should converge to the exact solution.

The substitution of this expansion into equation (3) identifies the intensity with the Laplace transforms of the indicial approximation

$$\mu I(1/\mu) = \sum a_j f_j(1/\mu). \quad (6)$$

Intensity observations at  $n$  discrete directions enable one to determine  $n$  coefficients of the temperature expansion, equation (4), as the solution of the linear simultaneous equation set

$$\mu_i I(1/\mu_i) = \sum_j f_{ij} a_j, \quad i = 1, 2, \dots, n. \quad (6)$$

A variety of different function classes have been used in inversion attempts. Examples are power series (King, unpublished), exponential functions (King, 1964), and various orthogonal sets such as Legendre, Chebyshev, or Laguerre polynomials (Yamamoto, 1961). All these

expansions share a common defect rendering them unsuitable for the inversion procedure. By choosing a particular finite polynomial expansion we restrict the form of the thermal profile.

Standing in contrast to this analytic procedure in which the temperature is broken down into components, is the synthetic method which approximates the profile by isothermal slabs. This is expressed by expanding the lapse rate in a sum of delta functions

$$\frac{dB(\tau)}{d\tau} = \sum (\Delta B)_j \delta(\tau - \tau_j). \tag{7}$$

Proceeding as before, the substitution of this slab approximation into the transfer equation yields the equation set

$$I(1/\mu) - B(0) = \int_0^\infty \frac{dB(\tau)}{d\tau} e^{-\tau/\mu} d\tau = \sum (\Delta B)_j e^{-\tau_j/\mu}. \tag{8}$$

We have not specified the slab boundaries  $\tau_j$ . Heretofore these positions have been assigned in advance, usually at significant levels in the atmosphere where lapse-rate discontinuities are anticipated (Kaplan, 1959; Wark, 1961).

Once again a knowledge of the intensity profile at the  $n$  directions  $\mu_i$  leads to a linear equation set determining the slab temperatures at  $n$  preset intervals

$$I(1/\mu_i) - B(0) = \sum_j (\Delta B)_j \exp(-\tau_j/\mu_i). \tag{9}$$

As we shall see this synthetic method is extremely sensitive to the choice of slab boundaries. As with the analytic procedure, the same criticism holds. The choice of  $\tau_j$  is critical, forcing in advance a particular structure on the slab profile.

We propose, therefore, a variable or floating slab method which determines uniquely the slab strengths and thicknesses for a given intensity profile. Consider equation (9). With the substitution  $x_j = \exp(-\tau_j)$  we succeed to a set of nonlinear simultaneous equations each of degree  $1/\mu_i$

$$I(1/\mu_i) - B(0) = \sum_j (\Delta B)_j x_j^{1/\mu_i}. \tag{10}$$

By choosing the sequence of viewing directions

$$\frac{1}{\mu_i} = i = 0, 1, 2, \dots, 2n-1, \tag{11}$$

we obtain the equation set of successively higher degree

$$\alpha_i = \sum_j a_j x_j^i, \quad i = 0, 1, 2, \dots, 2n-1, \tag{12}$$

where we have written  $\alpha_i = I(i) - B(0)$  and  $a_j$  for  $(\Delta B)_j$ .

The equation set arises in the construction of quadrature formulas of the Gaussian type (Lanczos, 1956; Kopal, 1961). Despite its nonlinearity the set is soluble uniquely by an elegant algorithm given, for example, by Chandrasekhar (1950) which consists of three steps. First,  $n$  auxiliary constants  $c_i$  are determined from the linear equation set

$$\alpha_{i+n} + \sum_{l=0}^{n-1} c_l \alpha_{i+l} = 0, \quad i = 0, 1, \dots, n-1. \tag{13}$$

The slab boundaries  $\tau_j = -\ln x_j$  are then obtained as the  $n$  roots of the equation

$$x^n + \sum_{l=0}^{n-1} c_l x^l = 0. \tag{14}$$

The knowledge of the roots enables one to determine the weights  $a_j$  from the first  $n$  equations of the set (12).

The solution admits the interpretation: Given  $n$  isothermal slabs, the  $a_j$  and  $\tau_j = -\ln x_j$  are the unique choice of slab weights and thicknesses fitting the  $2n$  intensity observations.

Fig. 1 displays three and five slab atmospheres inferred from intensity values of the following model atmosphere

$$I(1/\mu_i) = \frac{\mu_i}{\mu_i + 1}, \quad \frac{1}{\mu_i} = \begin{cases} 0, 1, \dots, 5 \\ 0, 1, \dots, 9 \end{cases} \tag{15}$$

The solid curve is the exact solution obtained directly by inversion

$$B(\tau) = \frac{1}{2\pi i} \int_{\gamma-i\infty}^{\gamma+i\infty} \mu I(1/\mu) e^{\tau/\mu} d(1/\mu) = 1 - e^{-\tau}. \tag{16}$$

The slab approximation is impressive. Note that the slab thickness is smallest in the region of greatest slope, thus minimizing the "cornering" error.

For comparison the same ten intensity values were used to infer the ten weights of slabs bounded at the ten present intervals

$$\tau_j = 0.1, 0.2, \dots, 1.0. \tag{17}$$

The thermal structure inferred by solving the equation set (9) for this model is grossly unrealistic (see Table 1).

The superiority of the floating over the fixed slab method can be understood by its relation to quadrature formulas. The Gaussian quadrature method achieves more accuracy than the preset Newton-Cotes intervals by allowing the integrand thicknesses to vary. Similarly in our inverse problem we have the additional degree of freedom in the determination of the slab boundaries as the unique solution of equation (14).

A second, more complicated atmospheric thermal

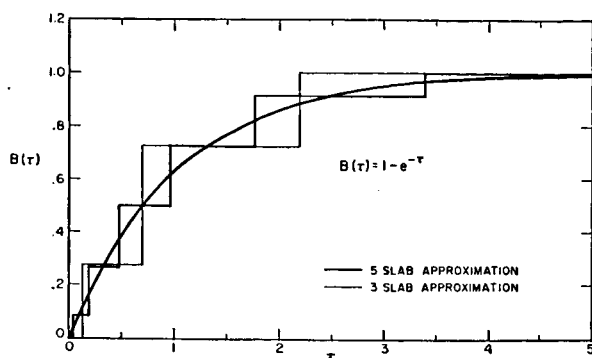
FIG. 1. Thermal structure inference for  $B(\tau) = 1 - e^{-\tau}$ .

TABLE 1. Thermal profile for constant thickness slabs.

$\tau$	$B(\tau)$
0-0.1	0
0.1-0.2	-82
0.2-0.3	+672
0.3-0.4	-1314
0.4-0.5	-1331
0.5-0.6	+3167
0.6-0.7	+2853
0.7-0.8	-4851
0.8-0.9	-1250
0.9-1.0	+2109
>1.0	0

profile is inferred in Fig. 2 using the ten intensity values

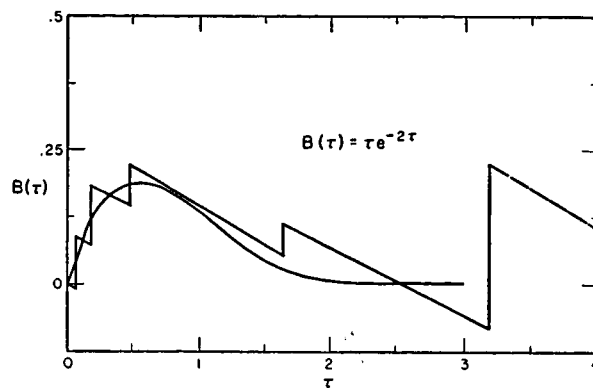
$$I(1/\mu_i) = \frac{\mu_i}{(\mu_i + 2)^2}, \quad \frac{1}{\mu_i} = 1, 2, \dots, 10. \quad (18)$$

The agreement of the inferred slab model to the exact solution

$$B(\tau) = \tau e^{-2\tau} \quad (19)$$

is remarkable for optical depths less than  $\tau \approx 1$ . For large values of optical depth the divergence is expected since even the deepest sensing ( $\mu_i = 1$ ) gives little information on the atmosphere beyond unit optical depth.

The constant slab slope ( $dB/d\tau = -0.14$ ) in Fig. 2 arises from the stipulation that the weights  $(\Delta B)_i$  in the Gaussian quadrature formula (10) be positive (Kopal, 1961). This requirement can always be satisfied by

FIG. 2. Thermal structure inference for  $B(\tau) = \tau e^{-2\tau}$ .

adding a constant slope to the lapse-rate which is subsequently subtracted after the inversion operation.

In a forthcoming paper "Meteorological Inferences from Satellite Radiometry, II" this floating slab method will be applied to thermal inferences of synthetic atmospheric models. An extension of the formalism to treat arbitrary band transmittance kernels is planned. The implications of the technique for the error analysis of raw radiometric data will be discussed.

*Acknowledgments.* Discussions with Dr. E. T. Florance were helpful in the formal aspects of the problem. All computations were performed by Mr. Richard Harrison.

This research was supported by the NASA Goddard Space Flight Center under Contract NAS5-3352.

#### REFERENCES

- Chandrasekhar, S., 1950: *Radiative transfer*. Oxford University, 393 pp.
- Kaplan, L. D., 1959: Inference of atmospheric structure from remote radiation measurements. *J. opt. Soc. Amer.*, **49**, 1004-1007.
- King, J. I. F., 1964: Greenhouse effect in a semi-infinite atmosphere. *Icarus*, in press.
- Kopal, Z., 1961: *Numerical analysis*. 2nd Ed., New York, John Wiley, 594 pp.
- Lanczos, C., 1956: *Applied analysis*. New York, Prentice-Hall, 539 pp.
- Wark, D. Q., 1961: On indirect temperature soundings of the stratosphere from satellites. *J. geophys. Res.*, **66**, 77-82.
- Yamamoto, G., 1961: Numerical method for estimating the stratospheric temperature distribution from satellite measurements in the CO<sub>2</sub> band. *J. Meteor.*, **18**, 581-588.